MOLECULAR AND CELLULAR BIOLOGY, Feb. 1995, p. 731–741 Vol. 15, No. 2
0270-7306/95/$04.00+0

p34^{Cdc28}-Mediated Control of Cln3 Cyclin Degradation

JULIA YAGLOM,[1] MAARTEN H. K. LINSKENS,[2]† SETH SADIS,[1] DAVID M. RUBIN,[1] BRUCE FUTCHER,[2] AND DANIEL FINLEY[1]*

Department of Cell Biology, Harvard Medical School, Boston, Massachusetts 02115,[1] *and Cold Spring Harbor Laboratory, Cold Spring Harbor, New York 11724*[2]

Received 21 September 1994/Returned for modification 3 November 1994/Accepted 15 November 1994

Cln3 cyclin of the budding yeast *Saccharomyces cerevisiae* is a key regulator of Start, a cell cycle event in G_1 phase at which cells become committed to division. The time of Start is sensitive to Cln3 levels, which in turn depend on the balance between synthesis and rapid degradation. Here we report that the breakdown of Cln3 is ubiquitin dependent and involves the ubiquitin-conjugating enzyme Cdc34 (Ubc3). The C-terminal tail of Cln3 functions as a transferable signal for degradation. Sequences important for Cln3 degradation are spread throughout the tail and consist largely of PEST elements, which have been previously suggested to target certain proteins for rapid turnover. The Cln3 tail also appears to contain multiple phosphorylation sites, and both phosphorylation and degradation of Cln3 are deficient in a *cdc28*^{ts} mutant at the nonpermissive temperature. A point mutation at Ser-468, which lies within a Cdc28 kinase consensus site, causes approximately fivefold stabilization of a Cln3–β-galactosidase fusion protein that contains a portion of the Cln3 tail and strongly reduces the phosphorylation of this protein. These data indicate that the degradation of Cln3 involves *CDC28*-dependent phosphorylation events.

The progress of cells through the division cycle is subject to controls ensuring faithful duplication of genetic material and other cell components. In the budding yeast *Saccharomyces cerevisiae*, environmental signals such as nutrient status are monitored in the central control step of the cell cycle, known as Start (35). Cell growth and division are coordinated by regulating the timing of this event. Upon the execution of Start, cells become irreversibly committed to division. An analogous G_1 event resulting in irreversible commitment to cell division has been described for mammalian cells and is known as the restriction point (33). Traversal of mammalian cells through the restriction point may involve the accumulation of unstable G_1 cyclins (6).

The timing of Start in yeast cells is controlled principally by Cln1, Cln2, and Cln3 (31). Each of these proteins contains a sequence motif conserved among all cyclins, which is thought to mediate their association with the cell cycle regulatory kinase Cdc28 (the cyclin box [14, 30]). Physical interaction with and activation of Cdc28 have been documented for all three Cln proteins (5, 48, 52). Cln3 differs dramatically from Cln1 and Cln2 in several respects. It is approximately 20- to 100-fold lower in abundance than Cln1 and Cln2 (47) and appears to lack the distinctly periodic expression of Cln1 and Cln2 (5, 47, 52). Nonetheless, *cln3* deletion mutants have more pronounced cell cycle defects than do *cln1* and *cln2* mutants (47).

Recent experiments suggest that the primary function of Cln3 is to induce *CLN1*, *CLN2*, and perhaps other genes (23, 47). Thus, Cln3 appears to play a critical but indirect role in Start. Accumulation of Cln1 and Cln2 is apparently necessary for the subsequent expression of *CLB1* to *CLB4*, which function in later stages of the cell cycle, particularly mitosis (1). Thus, Cln3 may serve as the initiator of a cascade of cyclin induction events. In controlling the initiation of this pathway, Cln3 coordinates cell growth and division.

The transcriptional controls that regulate all other known cyclin genes have not been observed for *CLN3*. However, the Cln3 protein is highly unstable, and mutations that stabilize Cln3 cause small cell size and precocious entry into S phase (30, 48). The short half-life of Cln3 may allow its steady-state abundance to be regulated rapidly and sensitively by changes in growth rate, protein synthesis, and cell size. Thus, the instability of Cln3 may underlie the ability of cells to adapt rapidly to fluctuating growth conditions and to avoid undergoing cell division under adverse conditions. The instability of Cln3 and perhaps its mammalian homologs therefore appears to be fundamental to their roles in coordinating cell growth and division.

Transferable signals for degradation have been identified in a number of short-lived proteins (12, 19, 24, 26). Here we characterize the degradation signal in Cln3 and show that it targets Cln3 for ubiquitin-dependent proteolysis. Ubiquitin serves as a marker for the degradation of many proteins in eukaryotes (8, 16, 21, 50). Cln3 apparently provides the first example of a signal for ubiquitin-dependent degradation composed primarily of PEST sequences. Such sequences, enriched in proline (P), glutamate (E), serine (S), and threonine (T), are present in a variety of short-lived proteins and have been proposed to target these proteins for turnover (37). The Cln3 degradation signal appears to be relatively complex; even a minimal signal consists of several critical elements and may require more than 80 amino acids. In particular, phosphorylation of the Cln3 degradation signal appears to be critical for its recognition. On the basis of the results below, we propose that PEST sequences involved in degradation function to couple phosphorylation with ubiquitination. The phosphorylation events implicated in Cln3 degradation are dependent on Cdc28 kinase, which physically associates with Cln3. Thus, Cln3 may be negatively regulated by the same cell cycle machinery that it activates.

MATERIALS AND METHODS

Yeast media and genetic techniques. Standard techniques were used for strain construction, transformation, and tetrad dissection (38). Cultures were grown at 30°C unless otherwise indicated. YPD medium consisted of 1% yeast extract, 2%

* Corresponding author. Mailing address: Department of Cell Biology, Harvard Medical School, 25 Shattuck St., Boston, MA 02115. Phone: (617) 432-3492. Fax: (617) 432-1144.
† Present address: Geron Corporation, Menlo Park, CA 94025.

Bacto Peptone, and 2% glucose. Synthetic media consisted of 0.7% Difco yeast nitrogen base supplemented with amino acids and uracil as described previously (38) and 2% glucose. Adenine was also used as a supplement when appropriate. For galactose induction, the same media were used except that methionine, uracil, and glucose were omitted and 2% galactose, 2% glycerol, 2% ethanol, and 40 μg of aspartate per ml, or alternatively 3% galactose and 2% raffinose, were added, as indicated.

Yeast strains. Unless otherwise indicated, experiments were carried out with the previously described (9) strain SUB62 (*MAT***a** *ura3-52 leu2-3,112 lys2-801 his3-Δ200 trp1-1*[*am*]), which also served as the congenic control strain in experiments involving ubiquitin-conjugating (Ubc) enzyme mutants (with the exception of the *ubc8* mutants [36]). *cdc34-1* (KY201), *cdc34-2* (KY203), and congenic control (KY130; *MAT***a** *bas1-2 bas2-2 ura3-52 leu2-Δ1 gcn4-Δ ade8*::*GCN4*) strains were supplied by D. Kornitzer. The *cdc28-4* strain (FC10-29) and congenic control (FC12-18; *MAT***a** *bar1 trp1 leu2 ura3 his2 ade1*) were supplied by F. Cross. The *pre1-1 pre1-4* mutant (yHI29/14) and congenic control (yHI29/W; *MAT***a** *ura3 leu2 his3*) strains were from D. Wolf.

Construction of deletions in the chromosomal *CLN3* gene. Standard techniques were used for manipulation and sequencing of DNA (40). A linker with appropriate restriction sites and termination codons in each reading frame was cloned into a derivative of plasmid pBF30 (30) immediately before the *CLN3* stop codon to yield an open reading frame ending in the sequence **CGC**AGCG GCCGCAGATCTCGAGGTACCGTCGACTGATTAATTAGCGCCGC**TGA** (plasmid pBF+) (bases in boldface type are derived from wild-type *CLN3*). Exonuclease III was used to generate nested unidirectional deletions (40) within the linker. Mutants were characterized by restriction mapping and sequencing (see Fig. 3). For selected mutants, a triple hemagglutinin (HA) epitope (7, 47, 48) was then cloned into a *Not*I site that had been placed in the *Sal*I site of the original linker. The genomic *CLN3* gene of strain W303a (*MAT*α *ura3 leu2 his3 trp1 ade2 can1*) was then replaced with a mutant *cln3* gene in two steps. First, the 1.4-kbp *Xho*I-to-*Hpa*I fragment at the *CLN3* locus was replaced with the *LEU2* gene by homologous recombination. The *LEU2* marker was then replaced by a *Pvu*II fragment of one of the mutant versions of pBF+, thus transferring a truncated version of *CLN3* to the chromosome. The *Pvu*II fragment carries a *URA3* marker upstream of *CLN3* (30). For measurement of protein half-lives, a *LEU2-GAL1* fragment was then inserted in place on the wild-type promoter by homologous recombination.

Construction of Cln3–β-Gal plasmids. All Cln3–β-galactosidase (β-Gal) constructions, including those of deletion variants, involved cloning PCR fragments into the *Bam*HI site of pLGSD5 (2). The Cln3 sequence is thus inserted near the N terminus of the 45-residue LacI-derived sequence which is joined to β-Gal (2). The Cln3M-expressing plasmid described in reference 48 was used as the template for all PCR experiments. 5′ endpoints of *CLN3* derived inserts extending to codon 404 correspond to the synthetic *Bam*HI site of this plasmid.

Construction of plasmids expressing Cln3-HA from the *CUP1* promoter. The Cln3M-expressing plasmid (48) was used as template for PCR of the entire 1.7-kbp *CLN3* open reading frame. Cln3M, which is identical to Cln3-HA used in this work, carries a triplicated HA tag inserted between residues 403 and 404 of Cln3. The sense oligonucleotide carried an *Eco*RI site 5′ to the ATG, and the antisense oligonucleotide carried a *Kpn*I site 3′ to the stop codon. The 1.7-kbp PCR fragment was digested with *Eco*RI and *Hin*dIII (at the natural *Hin*dIII site of Cln3), producing a 700-bp 5′ fragment. A 1-kbp 3′ fragment was produced by digestion with *Hin*dIII and *Kpn*I. From the *TRP1*-marked vector Yep96 (10), we prepared a 5.5-kbp *Bam*HI-*Kpn*I fragment and a 430-bp *Bam*HI-*Eco*RI fragment. These four fragments were ligated to produce plasmid Ye17, which expresses Cln3 from the *CUP1* promoter. The sequence of the entire *CLN3*-HA open reading frame was confirmed by sequencing. For transformation into Trp^+ strains, the 2.1-kbp *Bam*HI-*Kpn*I fragment from Ye17 was subcloned into the *LEU2*-marked vector YEplac181 (11).

Measurement of Cln3 half-life by immunoblotting. Measurement of Cln3 half-life has been described previously (48). Briefly, cells containing *GAL-CLN3* constructs were grown in YEP-galactose (1% yeast extract, 2% Bacto Peptone, 2% galactose) for 24 h to a density of 0.5×10^7 cells per ml. Glucose was added to 2% to repress the *GAL* promoter, and samples were taken at intervals. Northern (RNA) analysis was used to confirm that *CLN3* mRNAs for all mutants had disappeared within 7 min of glucose addition. Equal loading of total protein in each lane was confirmed by using anti-β-tubulin antibody (a gift of F. Solomon). Reaction of monoclonal antibody 12CAS with the triple HA epitope was visualized by an enhanced chemiluminescence system (Amersham). Multiple exposures were used to find the range within which the response of the film was linear. Exposures within the linear range were scanned with a Molecular Dynamics densitometer, and the half-life and relative abundance were determined for each protein.

Measurement of Cln3-HA and Cln3–β-Gal half-life by pulse-chase analysis. Pulse-chase procedures, cell lysis, immunoprecipitations, and gel electrophoresis were carried out essentially as described previously (10). ^{35}S-amino acids (Tran^{35}S-label) were from ICN. The addition of a variety of phosphatase inhibitors to the immunoprecipitation buffer was found to have no effect on the recovery of phosphorylated Cln3–β-Gal. The duration of labeling was 5 min in all pulse-chase experiments. Cln3–β-Gal half-life measurement was carried out with the synthetic media described above following 2 or more h of galactose induction. For pulse-chase analysis of Cln3-HA, cells were grown in appropriately selective synthetic media with 2% glucose in place of raffinose. Exponentially growing cells were induced with 0.1 mM $CuSO_4$ for 6 h and pulse-labeled. In experiments involving temperature-sensitive mutants, cells were grown at room temperature, shifted to 37°C after 6 h in the presence of $CuSO_4$, and pulse-labeled 30 min later. Half-life values were determined with a Molecular Dynamics PhosphorImager as described previously (10).

$^{32}P_i$ labeling. Phosphate labeling was carried out with YEP depleted of P_i (YEP-P) as described previously (51), supplemented with appropriate carbon sources. For phosphate labeling of β-Gal derivatives, cells were grown to exponential phase in synthetic medium lacking uracil and supplemented with 2% galactose, 2% glycerol, 2% ethanol, and 40 μg of aspartate per ml. Cells were harvested by centrifugation, washed three times with distilled H_2O, and resuspended in YEP-P supplemented with 2% galactose, 2% glycerol, 2% ethanol, and 40 μg of aspartate per ml. After 4 h, 0.1 to 0.3 mCi of $^{32}P_i$ was added to the medium, and incubation was continued for 40 min. Cells were then processed for immunoprecipitation as described above.

For $^{32}P_i$ labeling of Cln3-HA, cultures were grown to exponential phase in synthetic medium lacking leucine and methionine. $CuSO_4$ was then added to 100 μM, and incubation was resumed for 3 h. Cells were harvested and washed as described above, then resuspended in YEP-P supplemented with 100 μM $CuSO_4$ and 2% glucose, and incubated for an additional 2 h. The culture temperature was then shifted to 37°C; after an additional 30 min, 1.5 mCi of $^{32}P_i$ was added to each 8-ml culture, and labeling was carried out at 37°C for 25 min.

RESULTS

Construction and analysis of a nested set of Cln3 deletions. Sequences important for degradation of Cln3 were identified by making a set of nested deletions from the 3′ end of the *CLN3* open reading frame. For biochemical analysis, many of the Cln3 deletions were tagged with the HA epitope at their C termini. Constructs were placed under control of either the *CLN3* or *GAL* promoter and transplaced back into the yeast genome, replacing the wild-type copy of *CLN3*.

The effects of the mutations on protein half-life were assayed in two ways. First, the half-life of Cln3 overexpressed from the *GAL* promoter was determined directly, by measuring Cln3 abundance at different times after shutting off the *GAL* promoter (Fig. 1C and 2A). Second, the steady-state abundance of Cln3 protein expressed from either the *GAL* or *CLN3* promoter was determined by immunoblot analysis (Fig. 1C, 2B, and 2C). Assuming constant synthesis, the abundance of each mutant protein should be inversely proportional to the decay constant. The results of these two assays were in excellent agreement with one another: mutations causing increased half-life caused expected increases in steady-state protein abundance (Fig. 1 and 2). These experiments demonstrated that deletions throughout the Cln3 tail lead to stabilization of the protein (see below).

To test for phenotypic effects of Cln3 stabilization, the cell volume of each mutant was measured with a Coulter Channelizer (30). Cell volume is closely related to the level of Cln3 protein: as the amount of Cln3 in the cell increases, mode cell volume decreases (4, 30, 47). Thus, mutations increasing the stability of Cln3 protein decrease cell size. Conversely, mutations decreasing the specific activity of Cln3 increase cell size. This is an important assay because it can monitor the in vivo activity of untagged Cln3 expressed from its own promoter. This assay was done with both tagged and untagged versions of each mutant gene (Fig. 3B). In general, the C-terminal tag caused a slight increase in mode cell volume (presumably due to a slight destabilization of Cln3).

Deletion of the Cln3 tail (amino acids 404 to 580), which stabilized the protein, conferred a small-cell phenotype, as previously observed (30) (Fig. 3B). Deletions that extend beyond the tail resulted in a large-cell phenotype, presumably because they inactivate Cln3. For deletions within the tail, the cell volume assay was in good agreement with measurements of half-life and abundance of Cln3 except in the case of the three smallest C-terminal deletions (526, 514, and 478).

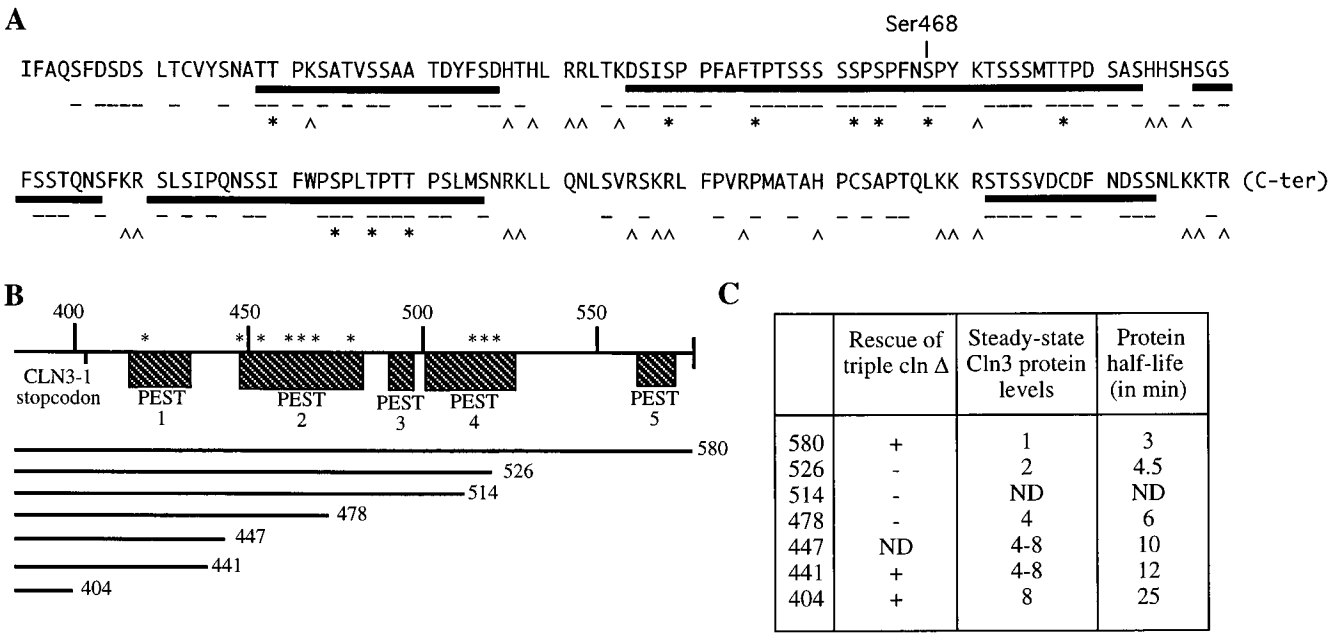

	Rescue of triple cln Δ	Steady-state Cln3 protein levels	Protein half-life (in min)
580	+	1	3
526	-	2	4.5
514	-	ND	ND
478	-	4	6
447	ND	4-8	10
441	+	4-8	12
404	+	8	25

FIG. 1. Deletion mapping of sequences involved in Cln3 degradation. (A) Sequence of Cln3 from amino acids 401 to 580 (the C terminus). P, D, S, and T residues are underlined. Five PEST regions (PEST 1 [amino acids 419 to 436], PEST 2 [amino acids 446 to 483], PEST 3 [amino acids 488 to 497], PEST 4 [amino acids 501 to 525], and PEST 5 [amino acids 562 to 574]) are indicated by heavy black bars. Asterisks indicate potential Cdc28 phosphorylation sites (SP or TP) (34); "Ser468" marks the sole site within the tail that satisfies the stringent consensus sequence (S/T-P-X-K/R) for Cdc28 phosphorylation (29, 34). Carets mark basic amino acids (H, K, and R). (B) Schematic drawing of C-terminal truncations. The top bar shows the PEST regions and potential Cdc28 phosphorylation sites (*). The number for each truncation mutant refers to the last Cln3 residue present. *CLN3-1* is a nonsense mutation causing complete loss of the tail sequence (30) and small cell size (45). (C) Summary of gene function, protein abundance, and protein half-life for the full-length protein and six truncation mutants expressed from the *GAL* promoter. ND, not determined.

In the exceptional mutants, cell volume increased (indicating a decrease in *CLN3* activity), despite an increase in Cln3 protein levels. In single copy, these three mutant genes were unable to complement a *cln1 cln2 cln3* triple mutation (Fig. 1C); a fourth mutant, 560, which lacks only the last 20 amino acids of Cln3, conferred a large-cell-size phenotype comparable to that of a *cln3* deletion (data not shown). However, when mutant genes 526, 514, and 478 were overexpressed from the *GAL1* promoter, they reduced the cell size, showing that they had some cyclin function (data not shown). Overexpression of these genes also resulted in complementation of the *cln1 cln2 cln3* triple mutation (data not shown). These results suggest that the last 20 amino acids of Cln3 are required for full activity; for example, they could constitute a localization signal. When the truncated proteins are stabilized or overexpressed, the increased quantity of Cln3 may compensate for its lowered specific activity. In summary, the biological activity of Cln3 can be perturbed by deletions throughout the Cln3 tail, as a result of effects on Cln3 stability and, in the case of the C-terminal 20 amino acids, Cln3 function.

Multiple PEST elements participate in Cln3 turnover. We define five PEST elements in the tail of Cln3, on the basis of the criteria of Rogers et al. (37) (Fig. 1). In general, there was a correlation between removal of PEST regions and stabilization of Cln3. Complete loss of the PEST-rich tail caused an eightfold increase in protein half-life and abundance and a 25% decrease in cell volume. A 32-amino-acid deletion of residues 490 to 522 (PEST 3 and PEST 4) increased half-life and abundance by about twofold (Fig. 2C and data not shown) and decreased cell size by about 8%. A nonoverlapping 34-amino-acid deletion of residues 449 to 483 (internal to PEST 2) increased protein half-life and abundance by about fourfold (Fig. 2C and data not shown) and decreased cell size by about 16%. However, little or no phenotype change resulted from deletion of amino acids 441 to 456 (Fig. 3B), which encompasses two potential Cdc28 phosphorylation sites and removes the N-terminal part of PEST 2. A critical portion of PEST 2 must therefore lie between amino acids 457 and 483.

Although PEST 2 is an important determinant of instability, all five PEST elements are in domains contributing to Cln3 turnover (Fig. 1 and 2). Thus, the turnover of Cln3 is not due to a single small signal, functioning in an all-or-none fashion. Rather, there are multiple proteolytic signalling components spread throughout the PEST-rich tail.

A transferable signal for degradation in the Cln3 tail. To test whether the Cln3 tail contains a transferable degradation signal, this segment was fused to a stable protein, *Escherichia coli* β-Gal, and expressed in yeast cells (Fig. 4). The resulting Cln3(404-580)–β-Gal hybrid protein (Cln3–β-Gal) was highly unstable, being degraded with an initial half-life of approximately 15 min (see below). Using the same pulse-chase procedure as for Cln3–β-Gal, we observed a half-life of approximately 5 min for HA-tagged Cln3 (see below); thus, degradation of Cln3–β-Gal is approximately threefold slower than that of Cln3 itself. This result suggests that the determinants of Cln3 degradation are localized primarily, but not exclusively, within the Cln3 tail.

We further characterized the structure of the Cln3 degradation signal by deletion analysis of Cln3–β-Gal. The N-terminal half of the Cln3 tail (amino acids 404 to 488) conferred a 30-min half-life on β-Gal (Fig. 4; see also below). We do not know whether the C-terminal half of the tail is also sufficient to signal degradation, because β-Gal constructs containing either residues 489 to 580 or residues 489 to 561 of Cln3 are rapidly cleaved to release a fragment of approximately the size of β-Gal.

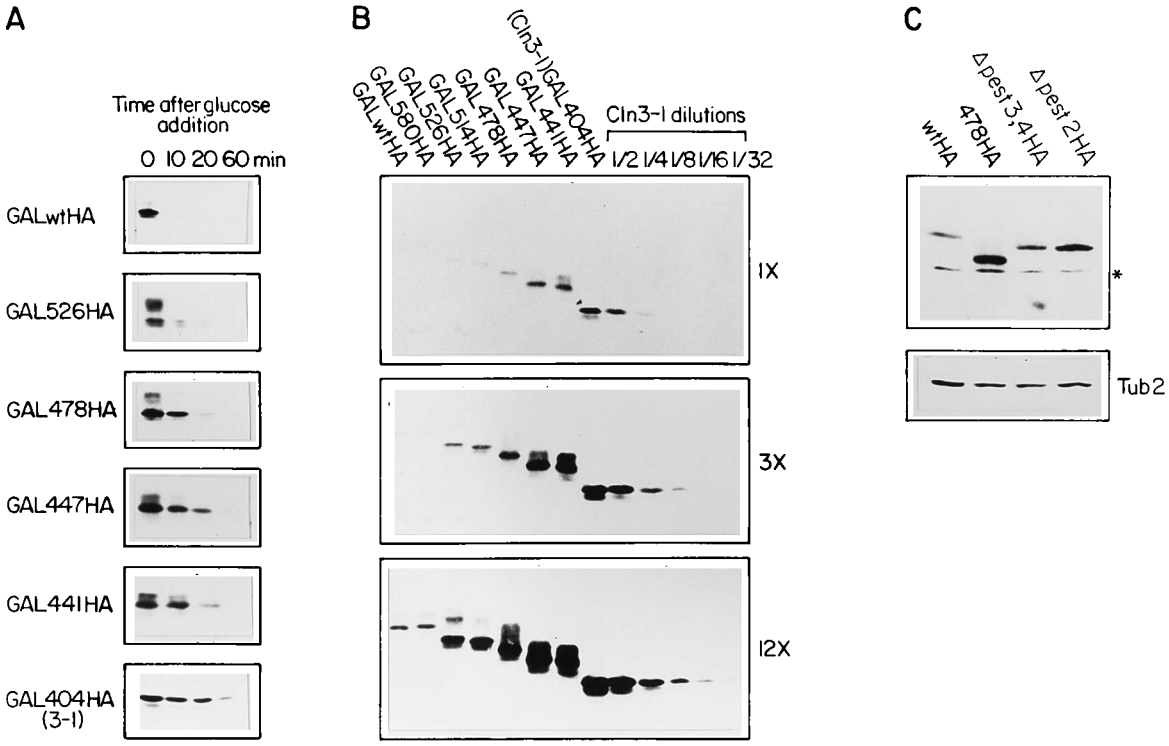

FIG. 2. Half-life and abundance of mutant Cln3 proteins. (A) Immunoblot analysis showing loss of Cln3 protein and its truncated derivatives with time after shutting off *GAL-CLN3* expression. "HA" indicates that the form of the protein tagged with the triple HA epitope (46, 47) was used. The electrophoretically retarded bands represent phosphorylated forms of Cln3 (data not shown; see also Fig. 8). (B) Steady-state Cln3 levels for a variety of HA-tagged mutant proteins expressed from the *GAL* promoter. 1×, 3×, and 12× refer to exposure times. Serial dilutions of tagged Cln3-1 extract were used to define the range within which the response of the enhanced chemiluminescence system was linear. GALwt(wild type)HA and GAL580HA differ by the presence of a C-terminal linker. The C-terminal sequences of these and all other constructs shown are given in Fig. 3C. In panels A and B, all visible bands are Cln3 derived. Essentially identical results were obtained for the deletion series with expression from the *CLN3* promoter (data not shown). (C) Steady-state protein levels for wild-type Cln3, the 478 truncation, and the two internal deletion mutant proteins, all tagged and expressed from the *CLN3* promoter. The asterisk indicates a nonspecific band cross-reacting with the anti-HA antibody. "Tub2" indicates β-tubulin used as a loading control.

Two nested sets of deletions were constructed from Cln3(404-488)–β-Gal (Fig. 4). All of these deletions stabilized the protein (Fig. 4). Thus, the minimal signal defined by this analysis consists of 85 residues. The size of the signal cannot be accounted for by the existence of two small, broadly spaced required elements, because not only terminal deletions (Cln3 [404-472]–β-Gal; Cln3[419-488]–β-Gal) but also an internal deletion (Cln3[404-436;458-488]–β-Gal) and a separate point mutation (Cln3[S468A]–β-Gal) caused stabilization (Fig. 4; see also below). Whether amino acids 404 to 488 comprise the smallest segment from the tail that can signal degradation could be established only by a more comprehensive set of deletions.

Deletion analysis of Cln3–β-Gal suggested the importance of PEST elements in the Cln3 degradation signal. The 85-residue minimal signal includes PEST 1 and 2 as well as a 16-residue segment N-terminal to PEST 1. Overall, the minimal signal is composed of 59% P, S, T, D, and E. Although PEST 2 alone is not sufficient to target β-Gal for degradation, it clearly plays a critical role within the context of Cln3(404-488)–β-Gal, because three nonoverlapping mutations within PEST 2 result in fourfold or greater stabilization (deletions of amino acids 437 to 457 and 473 to 488 and substitution of S468; Fig. 4; see also below).

When Cln3(404-488)–β-Gal was analyzed electrophoretically, two bands were observed (Fig. 4C). The retarded band was identified as a phosphorylated form by phosphatase digestion (Fig. 4D) and $^{32}P_i$-labeling experiments (Fig. 5). The N- or C-terminal deletions that stabilized the protein also reduced levels of phosphorylation (Fig. 4 and 6, Cln3[404-472]–β-Gal and Cln3[419-488]–β-Gal). Interestingly, two separate regions (404 to 436 and 457 to 488) are required for efficient phosphorylation. Between these two regions is a segment (amino acids 437 to 457) required for degradation but not for phosphorylation (Fig. 4B). The latter does not simply serve as a site of ubiquitin attachment in the fusion protein, because degradation of the fusion protein requires the well-described (50) ubiquitination sites in β-Gal, lysines 15 and 17. This was shown by substituting arginine residues at these positions, which resulted in complete stabilization of Cln3(404-488)–β-Gal (data not shown).

Cln3–β-Gal degradation is ubiquitin dependent. The pathway of Cln3–β-Gal degradation was initially investigated by using a mutant in the cytoplasmic protease known as the proteasome. The essential genes *PRE1* and *PRE4* encode subunits of this 20S complex (15, 18). Figure 7C shows that turnover of Cln3(404-580)–β-Gal was strongly inhibited in a *pre1-1 pre4-1* double mutant. Because the proteasome mediates degradation of ubiquitin-protein conjugates (15, 16, 43), this result suggested a role for ubiquitin in Cln3–β-Gal degradation.

Efficient degradation of many proteins requires the sequential ligation of ubiquitin molecules to the substrate to form a multiubiquitin chain linked through Lys-48 of ubiquitin (3, 8). An arginine substitution at this position (UbK48R) prevents chain formation and protein breakdown in vitro (3) and is lethal in *S. cerevisiae* (10). However, when UbK48R was over-

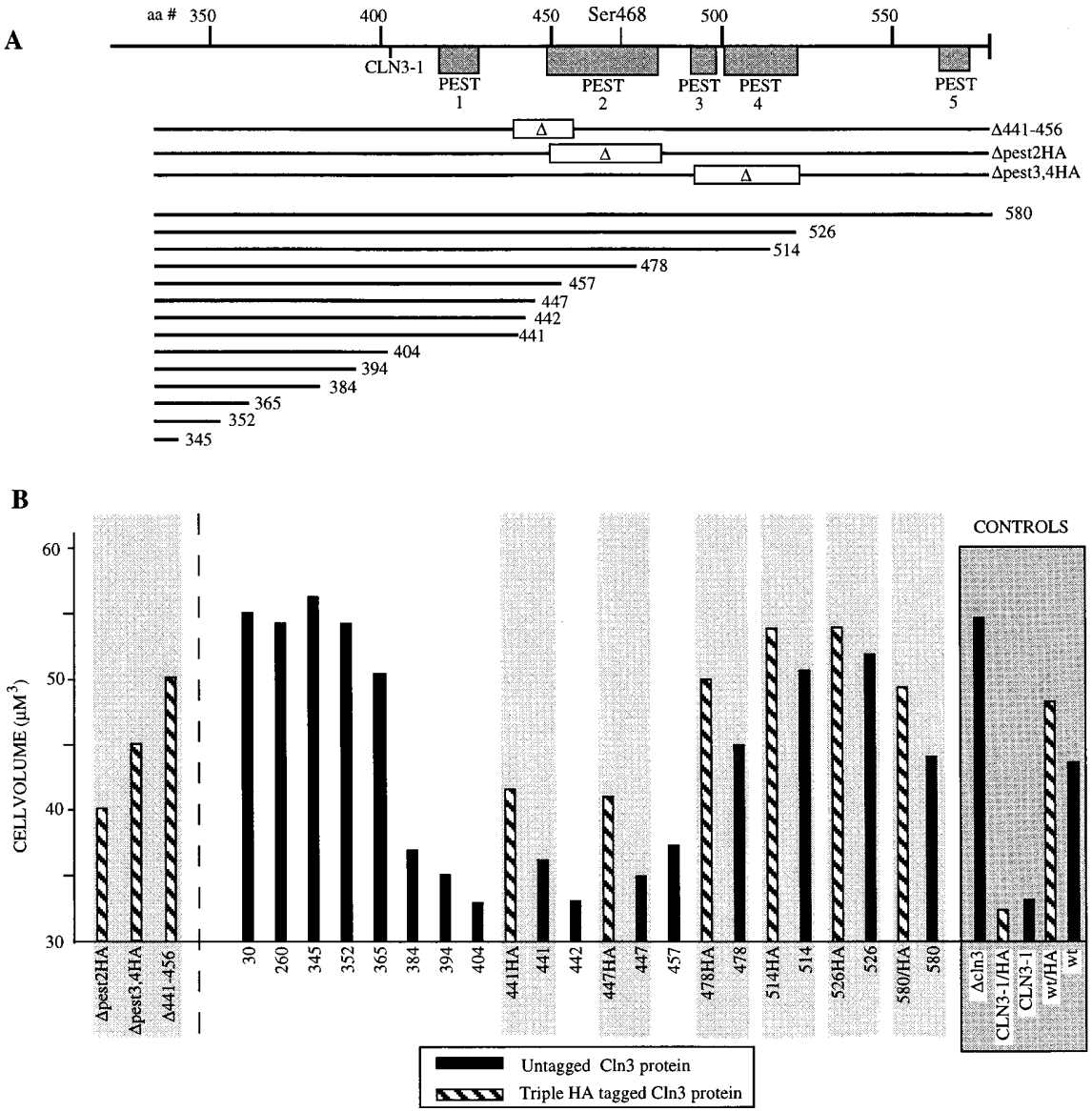

C

wt	570-NDSSNLKKTR
wtHA	570-NDSSNLKKTR***
CLN3-1	400-IFA
CLN3-1HA	400-IFA***
Δcln3	ΔΔΔ
580	570-NDSSNLKKTR**SGRRCGRID**
580HA	570-NDSSNLKKTR**SGRRC***GRID**
526	520-PSLMSN**SRCGRID**
526HA	520-PSLMSN**SRC***GRID**
514	510-FWPS**RCGRID**
514HA	510-FWPS**RC***GRID**
478	470-KTSSSMTT**RRCGRID**
478HA	470-KTSSSMTT**RRC***GRID**
457	450-PFAFTPTD
447	440-RRLTKDS**RCGRID**
447HA	440-RRLTKDS**RC***GRID**
442	440-RR**STD**
441	440-R**SRCGRID**
441HA	440-R**SRC***GRID**
404	400-IFAQ**TD**
394	390-SQEL**D**
384	380-QLKL**STD**
365	360-NSNK**TD**
352	350-FP**VD**
345	340-LLDIA**D**
260	250-AGTAINKSSS**TD**
30	20-GTSTATAASV**D**
Δ441-456	as wtHA, with Δ of aa 441-456
Δpest2HA	as wtHA, with Δ of aa 449-483
Δpest3,4HA	as wtHA, with Δ of aa 490-522
(3HA-tag) ***	GRIFYPYDVPDYAGYPYDVPDYA
	GSYPYDVPDYAAQC

FIG. 3. Phenotypic effects of Cln3 deletions. (A) Map of Cln3 deletions. aa, amino acid. (B) The mode of the cell volume distribution for various *CLN3* and *cln3* strains. Each result is the average of at least three independent determinations, which rarely deviated from each other by more than 2 μm^3. In all cases, the mutant *cln3* gene is integrated at the *CLN3* locus, expressed from the *CLN3* promoter, and is the only *CLN3* or *cln3* gene in the cell. wt, wild type. (C) C-terminal amino acid sequences of Cln3 derivatives, as predicted from DNA sequencing. Amino acids foreign to Cln3 are shown in boldface type and underlined. Asterisks indicate the triple HA epitope, whose sequence is given at the bottom.

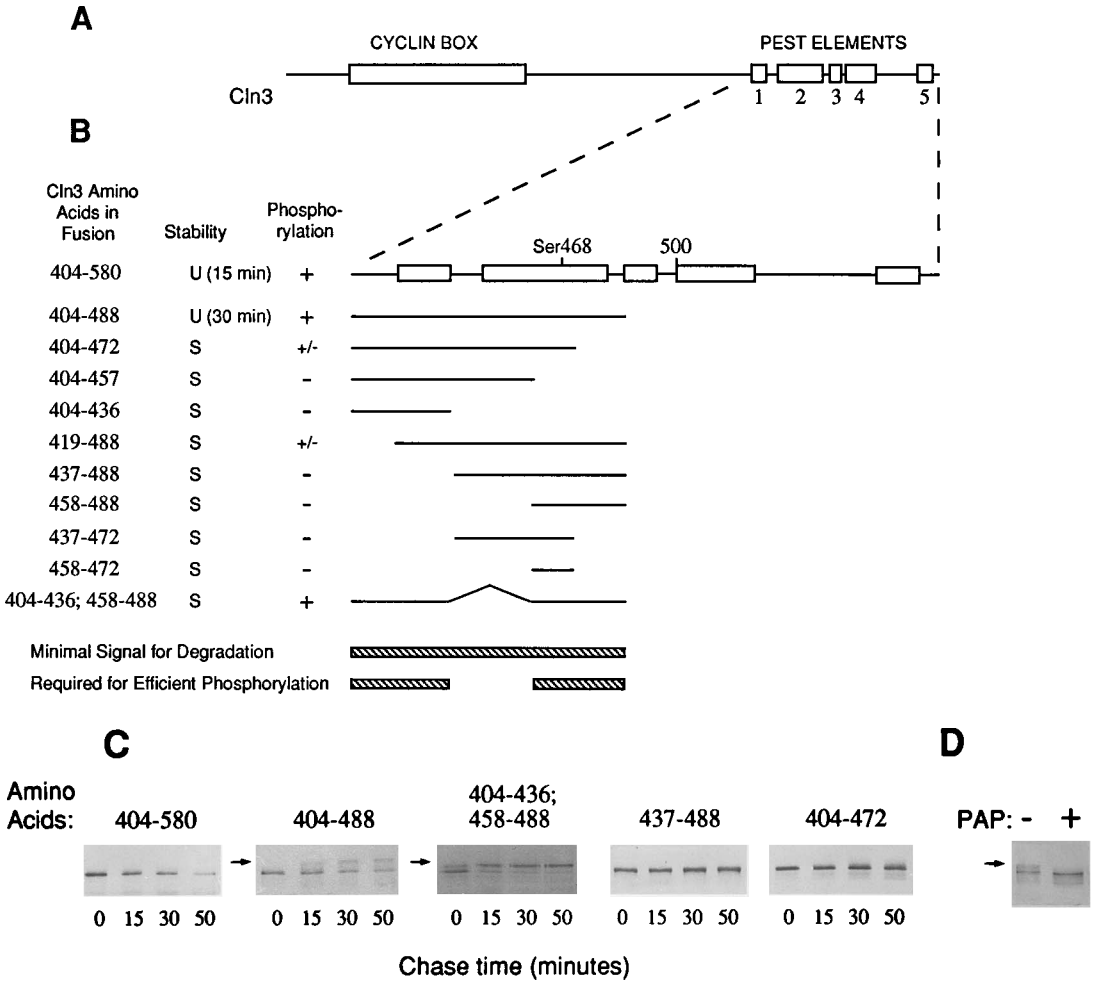

FIG. 4. Deletion analysis of Cln3–β-Gal. (A) Schematic representation of Cln3 showing the cyclin box and PEST elements. (B) Stability and phosphorylation of fusion proteins in which the indicated sequences from Cln3 are joined to the N terminus of β-Gal (see Fig. 7 and 9 for quantitation of half-lives). U, unstable; S, stable. (C) Pulse-chase experiments performed on specific derivatives of Cln3–β-Gal. Arrows indicate phosphorylated forms (see also Fig. 4D and 5 to 7 for phosphorylation of Cln3–β-Gal derivatives). (D) Treatment of Cln3(404-488)–β-Gal with potato alkaline phosphatase (PAP). The faint bands migrating more rapidly than full-length Cln3(404-488)–β-Gal are background bands from the immunoprecipitation. After cell lysis, the fusion proteins were immunoprecipitated with antibody to β-Gal, analyzed electrophoretically, visualized by fluorography, and quantitated. For all experiments involving Cln3–β-Gal derivatives, the reported half-life values are based on the pooled intensities of both phosphorylated and nonphosphorylated bands. For proteins designated as stable, no significant degradation could be detected with a 90-min chase. For Cln3–β-Gals with intermediate levels of phosphorylation indicated, the phosphorylated band could be detected only upon fluorographic overexposure (see Fig. 6). Phosphatase treatments were performed as described previously (48). We note that expression of the same C-terminal Cln3 fragment at the C terminus of β-Gal resulted in equivalent destabilization.

produced in yeast cells in the presence of wild-type ubiquitin, only a mild stabilization of Cln3(404-580)–β-Gal was observed (data not shown). The weakness of this effect may reflect removal of UbK48R from multiubiquitin chains by deubiquitinating enzymes and its replacement by wild-type ubiquitin (10).

To inhibit this putative editing process, the *UbK48R* mutation was combined with a mutation that interferes with deubiquitination, *UbG76A* (20). Glycine 76, the C-terminal residue of ubiquitin, is the site of ubiquitin attachment to ε-amino groups of protein lysine residues. Conjugation of the double-mutant ubiquitin to a nascent chain appears to inhibit both elongation and deubiquitination and thus results in a chain of relatively static length that is too short to signal degradation (10). Figure 7E shows that overexpression of UbK48R,G76A results in strong stabilization of Cln3(404-580)–β-Gal. Thus, the breakdown of this polypeptide appears to be ubiquitin dependent. Moreover, stabilization was accompanied by the

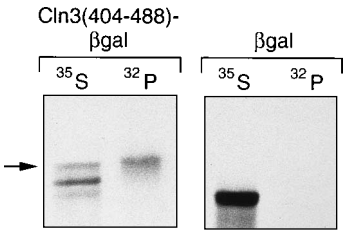

FIG. 5. The electrophoretically retarded form of Cln3(404-488)–β-Gal is phosphorylated. Cultures expressing either Cln3(404-488)–β-Gal or β-Gal with no Cln3-derived sequences were grown in synthetic medium and subcultured in either $^{32}P_i$ labeling medium or ^{35}S-amino acid labeling medium. Proteins were radiolabeled and analyzed as described in the legend to Fig. 4 and in Materials and Methods. The ratio of ^{32}P to ^{35}S counts per minute was approximately 50-fold greater for Cln3(404-488)–β-Gal than for β-Gal. No $^{32}P_i$-labeled band corresponding to the faster-migrating form of Cln3(404-488)–β-Gal was detectable. Autoradiographic overexposures showed that, in contrast, phosphorylation of β-Gal itself was not associated with an electrophoretic mobility shift (data not shown).

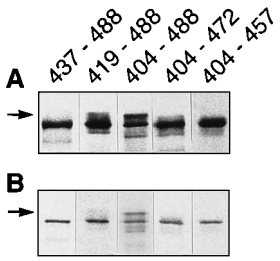

FIG. 6. Phosphorylation levels of Cln3–β-Gal fusion proteins. Proteins were pulse-labeled with ^{35}S-amino acids for 5 min and, after a 50-min chase incubation, analyzed by immunoprecipitation as described in the legend to Fig. 4. The numbers at the top refer to the Cln3-derived residues present in each fusion protein. The arrow designates phosphorylated forms. Panels A and B are taken from the same experiments but are derived from autoradiographic overexposures (A) and underexposures (B). Panel A illustrates that fusion proteins containing amino acids 419 to 488, 404 to 488, and 404 to 472 of Cln3 are phosphorylated, whereas panel B illustrates that the relative level of phosphorylation is highest for the fusion protein containing amino acids 404 to 488 of Cln3.

accumulation of a periodic array of high-molecular-weight Cln3–β-Gal derivatives, which could be visualized upon fluorographic overexposure (Fig. 7F). The spacing of these bands and their dependence upon overexpression of a mutant ubiquitin suggest that they represent progressively ubiquitinated forms of Cln3–β-Gal. A different modified form of Cln3–β-Gal accumulates to much higher levels upon overexpression of UbK48R,G76A (Fig. 7E). This band was found to disappear

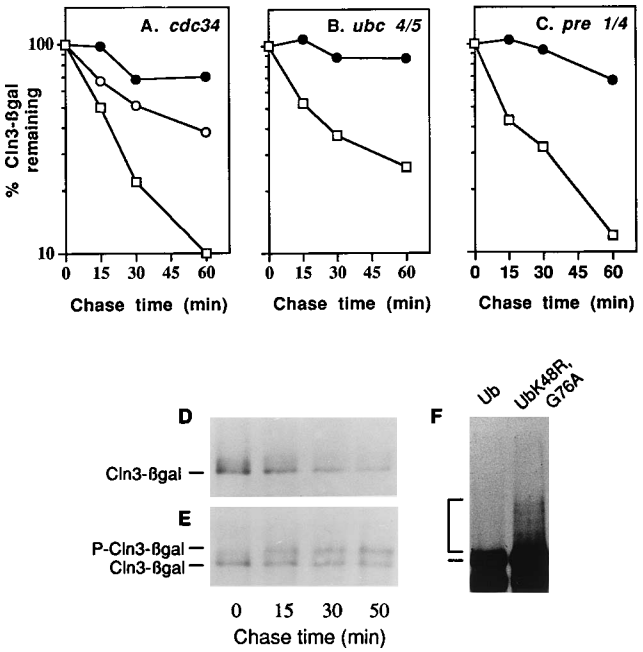

FIG. 7. Cln3(404-580)–β-Gal degradation proceeds through a specific ubiquitin-dependent proteolytic pathway. Degradation of Cln3(404-580)–β-Gal was measured by pulse-chase analysis in congenic sets of strains. (A) Open circles, *cdc34-1*; filled circles, *cdc34-2*. (B) Filled circles, *ubc4 ubc5*. (C) Filled circles, *pre1 pre4*. Wild-type strains are represented in all three panels by open squares. (D and E) Pulse-chase analysis of Cln3–β-Gal degradation in strains overexpressing either wild-type ubiquitin (D) or the UbK48R,G76A variant (E). "P-Cln3-βgal" indicates the position of phosphorylated Cln3. (F) Fluorographic overexposure of lanes comparable to time zero points of panels D and E. Brackets indicate the position of presumptive ubiquitin (Ub)–Cln3–β-Gal conjugates. Experiments were carried out at either 37°C (A and C) or 30°C (B, D, E, and F).

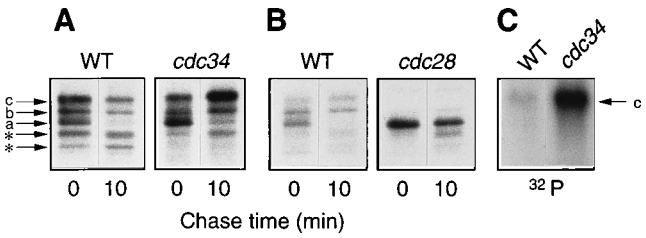

FIG. 8. Phosphorylation and degradation of Cln3-HA in *cdc34* and *cdc28* mutants. All experiments were done at 37°C. In panels A and B, cells were labeled with ^{35}S-amino acids as described in Materials and Methods. (A) Strains KY130 (wild type [WT]) and KY203 (*cdc34*). (B) FC12-18 (wild type [WT]) and FC10-29 (*cdc28*). (C) Radiolabeling was carried out with $^{32}P_i$ for 20 min. On the basis of relative stabilities and electrophoretic mobilities, we suggest that band a corresponds to p60 described in reference 5 (i.e., full-length Cln3), band b corresponds to p65, band c corresponds to p68, and the bands marked with asterisks correspond to p54 and p52, which decay less rapidly and appear to be partial breakdown products of Cln3 (5). The pooled intensities of bands a to c remaining after 10 min was 24% for KY130 (wild type), 82% for KY203 (*cdc34*), 51% for FC12-18 (wild type), and 89% for FC10-29 (*cdc28*). Standard deviations were 6, 19, 4, and 11%, respectively. The experiments in panels A and B were done independently three and four times, respectively. There was a reproducible difference in Cln3-HA stability between the two wild-type strains (KY130 and FC12-18), which was correlated with the level of Cln3-HA phosphorylation at the zero point. We note that in a previous study, the *cdc34-2* mutation appeared to cause no more than twofold stabilization of Cln3 (48). The stronger effect observed in the present study could be due to the use of different strains.

upon phosphatase treatment and thus represents a phosphorylated form of Cln3–β-Gal (data not shown; see also below).

Involvement of Ubc enzymes in Cln3–βgal degradation. Ubc enzymes are required for transferring ubiquitin to protein substrates (21). The various Ubc enzymes that have been identified in *S. cerevisiae* define distinct pathways of ubiquitin conjugation. Cln3–β-Gal was not stabilized in *ubc1*, *ubc2*, *ubc6*, *ubc7*, *ubc8*, or *ubr1* mutants (data not shown) (21, 50). In contrast, mutants with temperature-sensitive defects in the Ubc3 enzyme (Cdc34 [13]) exhibited strong stabilization of Cln3–β-Gal at the nonpermissive temperature (Fig. 7A). The stabilization of Cln3–β-Gal observed in *cdc34* mutants is attributable to the *cdc34* mutations, because Cln3–β-Gal was stabilized to a higher degree by the stronger of two *cdc34* alleles (Fig. 7A) and because transformation of these strains with a wild-type *CDC34* gene completely restored Cln3–β-Gal instability (data not shown). *cdc34* mutants arrest in late G_1 upon a temperature shift (13). However, the stabilization of Cln3–β-Gal does not appear to result from cell cycle redistribution, since stabilization was observed after 30 min at 37°C, whereas the doubling time of wild-type cells was greater than 4 h under these conditions.

The redundant pair of Ubc enzymes Ubc4 and Ubc5 (42), which are involved in degradation of a variety of short-lived and abnormal proteins but have not been implicated in cell cycle regulation, were also required for efficient Cln3–β-Gal degradation (Fig. 7B). Ubc3 and Ubc4/Ubc5 may therefore cooperate in the breakdown of Cln3–β-Gal. Experiments to determine whether degradation of native Cln3 is inhibited in *ubc4 ubc5* double mutants have been hindered by difficulties in pulse-labeling Cln3 in these severely growth defective strains.

Cln3 phosphorylation and degradation in *cdc34* mutants. To address the possible role of Cdc34 in degradation of native Cln3, we expressed full-length, HA-tagged Cln3 (48) from the *CUP1* promoter. When Cln3-HA was pulse-labeled and immunoprecipitated with antibody to the HA epitope, five electrophoretic bands were observed (Fig. 8A). These bands are not seen in samples from congenic control cells not expressing Cln3-HA (data not shown). Because all five bands can be

detected by immunoblotting, they appear to represent variant forms of Cln3-HA rather than coimmunoprecipitating proteins (data not shown). The pattern of five bands closely resembles that reported by Cross and Blake (5), using antibodies to native Cln3, and is thus unlikely to reflect artifactual consequences of epitope tagging. However, the bands marked by asterisks appear to be nonfunctional products of partial Cln3-HA breakdown (5). In wild-type cells, bands a, b, and c decay with exponential kinetics when quantitated as a group (data not shown). The characteristics of these bands are described below and in the legend to Fig. 8. Briefly, band a appears to represent full-length Cln3, and band b appears to represent a Cln3 variant that is modified but not phosphorylated, and band c appears to represent phosphorylated Cln3. Band c could be detected by in vivo $^{32}P_i$ labeling (Fig. 8C) and was also eliminated upon phosphatase treatment (data not shown).

Stabilization of Cln3 is clearly observed in *cdc34* mutants shifted to the nonpermissive temperature (Fig. 8A). In addition, $^{32}P_i$ labeling showed directly that the level of phosphorylated Cln3 is enhanced in *cdc34* mutants at the nonpermissive temperature (Fig. 8), consistent with previous observations (48). The enhanced phosphorylation is also reflected in an increase in the level of band c during the chase incubation in samples labeled with ^{35}S-amino acids (Fig. 8A). Prior to the chase incubation, no enhancement of band c is apparent in *cdc34* mutants, suggesting that the rate of Cln3 phosphorylation is not significantly affected by the *cdc34* mutation. Thus, the higher levels of phosphorylated Cln3 in this *cdc34* strain are largely due to stabilization of Cln3 or phosphorylated Cln3. The observation that both Cln3 and Cln3–β-Gal are stabilized in *cdc34* mutants shows that the fusion protein is degraded by a pathway the same as or similar to that of the native protein.

Ser-468-dependent phosphorylation implicated in Cln3 (404-488)–β-Gal turnover. As described above, the data in Fig. 4 to 8 are consistent with a role of phosphorylation in the degradation of Cln3–β-Gal. First, terminal deletions in the degradation signal of Cln(404-488)–β-Gal, which interfere with its phosphorylation, also inhibit degradation (Fig. 4 and 6). Second, the stabilization of Cln3–β-Gal was accompanied by accumulation of its phosphorylated form in UbK48R,G76A overexpressors, *cdc34* mutants, *ubc4 ubc5* mutants, and *pre1 pre4* mutants (Fig. 7E and data not shown). This was also observed for Cln3-HA in *cdc34* mutants (Fig. 8A). The accumulation of phosphorylated Cln3-HA and Cln3–β-Gal upon inhibition of degradation suggested that the phosphorylated forms may be intermediates in turnover and that phosphorylation may serve to target Cln3 for degradation.

This possibility was tested by introducing amino acid substitutions at candidate phosphorylation sites. The C-terminal portion of PEST 2, whose role in degradation was indicated by deletion analysis, contains the only stringent representation in the tail region of the consensus site for the Ser/Thr kinase Cdc28 (Ser-Pro-Tyr-Lys [29]). Substitution of this serine with alanine stabilized Cln3(404-488)–β-Gal approximately fivefold (Fig. 9A). The S468A substitution also resulted in a four- to fivefold-decreased abundance of the phosphorylated band (Fig. 9C) but did not eliminate it (data not shown), indicating the existence of at least one other phosphorylation site in the fusion protein. Stabilization of Cln3(404-580)–β-Gal (Fig. 9B) by the S468A mutation was approximately 1.5-fold, and the reduction in normalized levels of phosphorylation was approximately 2-fold. Thus, the effects of the S468A substitution on Cln3(404-580)–β-Gal phosphorylation and degradation are much less marked than on Cln3(404-488)–β-Gal. This attenuation of the S468A effect might reflect the existence of redundant, independently functioning degradation signals in the Cln3 tail, as suggested by the deletion analyses.

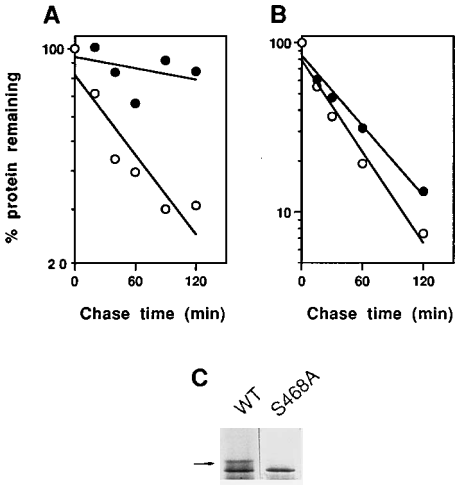

FIG. 9. Effect of a Ser-to-Ala substitution at residue 468 on the phosphorylation and degradation of Cln3–β-Gal derivatives. (A) Degradation of Cln3(404-488;S468A)–β-Gal (filled circles) and the wild-type control (open circles) at 30°C. Similar results have been obtained in five independent experiments. (B) Degradation of Cln3(404-580;S468A)–β-Gal (filled circles) and wild-type control (open circles) at 30°C. Similar results have been obtained in three independent experiments. (C) Cln3(404-488)–β-Gal phosphorylation following a 50-min labeling with ^{35}S-amino acids at 25°C. Equivalent results were obtained at 30°C and with shorter labeling times. The arrow indicates phosphorylated Cln3(404-488)–β-Gal. WT, wild type.

Role of Cdc28 in Cln3 phosphorylation and degradation. The results presented above led us to test whether Cln3–β-Gal degradation is dependent on Cdc28 kinase. At the permissive temperature, Cln3(404-488)–β-Gal was degraded at comparable rates in wild-type and *cdc28-4* mutant cells (data not shown). At the nonpermissive temperature, however, a fourfold stabilization of Cln3(404-488)–β-Gal was apparent in the mutant cells (Fig. 10A). Similar results were obtained with Cln3(404-580)–β-Gal (data not shown). Stabilization did not

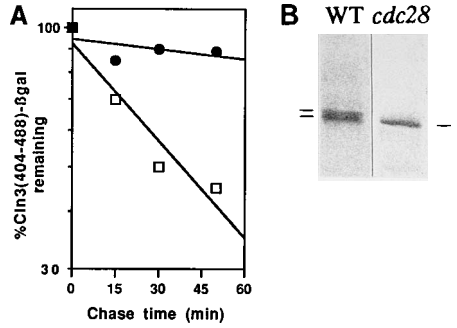

FIG. 10. Phosphorylation and degradation of Cln3(404-488)–β-Gal are *CDC28* dependent. (A) Degradation of Cln3(404-488)–β-Gal in *cdc28-4* (FC10-29; circles) and the congenic control (FC12-18; squares) strains. Cln3(404-580)–β-Gal degradation is similarly dependent on *CDC28* (data not shown). (B) *cdc28*-dependent phosphorylation of Cln3(404-488)–β-Gal. Cells growing exponentially at 25°C were shifted to 37°C for 2 h before labeling. The doubling time of FC12-18 at 37°C is 5 h. Galactose induction was carried out in the absence of alternate carbon sources overnight prior to pulse-labeling. Panel B is from a 5-min pulse-labeling with no chase incubation. Evidence that the retarded form of Cln3(404-488)–β-Gal corresponds to a phosphorylated species is presented in Fig. 4 and 5. The retarded form of Cln3(404-488)–β-Gal that is seen in samples from cells grown at 37°C is phosphatase sensitive (data not shown). However, the extent of electrophoretic retardation produced by phosphorylation was reproducibly greater at 30°C than at 37°C (in wild-type [WT] cells).

result from general inhibition of the ubiquitin pathway, since there was no stabilization of other ubiquitin-dependent substrates such as ubiquitin–K–β-Gal (data not shown) (50).

As described above, four distinct mutations affecting components of the ubiquitin-dependent proteolytic pathway caused both stabilization of Cln3–β-Gal and accumulation of its phosphorylated form. In striking contrast, stabilization of Cln3(404-488)–β-Gal in *cdc28* mutants at the nonpermissive temperature was accompanied by strongly decreased phosphorylation (Fig. 10B). This result indicates that Cln3(404-488)–β-Gal phosphorylation is *CDC28* dependent and is in agreement with point mutant analysis in suggesting a role for *CDC28*-dependent phosphorylation of Cln(404-488)–β-Gal in its degradation. Interestingly, these data also separate a determinant of *CDC28*-dependent Cln3 degradation from its cyclin box sequence (Fig. 4), which is thought to be required for Cdc28 binding and is absent from the Cln3–β-Gal fusions.

The relevance of the results presented above to native Cln3 was addressed by expressing Cln3-HA in *cdc28* mutants. After pulse-labeling with ^{35}S-amino acids at the nonpermissive temperature, the phosphorylated form of Cln3 described above, represented by band c, was undetectable (Fig. 8B). Cdc28 kinase activity is therefore required for Cln3 phosphorylation in vivo. Only band a was present at significant levels in *cdc28* mutants. This band is likely to correspond to p60 described in reference 5, because both bands accumulate in *cdc28* mutants and both occupy the same position in the electrophoretic ladder of Cln3 bands. p60 comigrates with full-length Cln3 (5). Thus, Cln3 accumulates in an unmodified form in *cdc28* mutants. After 10 min, approximately 50% of Cln3-HA was degraded in the wild-type strain, as opposed to 10% in *cdc28* mutants, indicating that the *cdc28* mutation leads to stabilization of Cln3 itself, similarly to Cln3–β-Gal. One interpretation of these data is that stabilization of Cln3 results from its failure to be phosphorylated.

DISCUSSION

Progress through the cell cycle is governed by an orderly succession of cyclin proteins. Accordingly, all known cyclins are rapidly degraded, either constitutively or in a temporally regulated fashion. Mitotic cyclin degradation is mediated by a short sequence known as the destruction box (12). The proteolytic machinery that acts upon mitotic cyclins is abruptly activated during specific phases of mitosis (12, 39) and remains active until the late G_1 phase of the subsequent cell cycle (1). Temporal regulation of mitotic cyclin degradation may be effected by $p34^{Cdc28/cdc2}$-dependent phosphorylation and activation of a ubiquitin-cyclin ligase (17). In addition, the dependence of cyclin A and B2 degradation on $p34^{Cdc28/cdc2}$ may reflect a requirement for the proteolytic substrate to be bound to $p34^{Cdc28/cdc2}$ (44, 49). There is no evidence to suggest that mitotic cyclin degradation involves Cdc28-dependent phosphorylation of cyclins themselves, nor do PEST elements appear to be involved in mitotic cyclin turnover. In these respects, and in its *CDC34* dependence, the mechanism and regulation of Cln3 cyclin degradation differ significantly from those of mitotic cyclins.

Cdc34 mediates degradation of Cln3. We have shown that Cln3 degradation is *CDC34* dependent and that phosphorylated forms of Cln3 accumulate in *cdc34* mutants largely as a consequence of Cln3 stabilization. Two other substrates of the Cdc34 (Ubc3) pathway have recently been identified, the transcription factor Gcn4 (24) and the Cdc28 kinase inhibitor Sic1 (41). The inability of *cdc34* mutants to degrade Sic1 appears to account for their conditional lethality and inability to enter S phase (41). Thus, although initially identified by virtue of its requirement for the G_1-to-S transition, Cdc34 now appears to mediate degradation of a variety of proteins, not all of which are involved in cell cycle control. All three presumptive substrates of Cdc34 contain PEST sequences and are phosphoproteins (24, 28, 32). On the basis of the results with Cln3, it is possible that phosphorylation-dependent degradation is a common feature of Cdc34 substrates.

A degradation signal in Cln3. The tail region of Cln3 functions as a degradation signal in that it is both necessary and sufficient for the *CDC28*-dependent, *CDC34*-dependent degradation characteristic of Cln3 itself. Within the tail region, many segments contribute to instability, as defined by deletion analysis of either Cln3 or Cln3–β-Gal fusion proteins. The results of these two deletion analyses are qualitatively congruent and thus consistent with the view that the proteolytic pathway for degradation of Cln3–β-Gal fusions reflects that of native Cln3.

The tail (or at least residues 404 to 488 of Cln3) is not a fully autonomous degradation signal, as Cln3–β-Gal turnover requires the presence of either Lys-15 or Lys-17 of the β-Gal component of the fusion protein. On the basis of observations with other β-Gal fusion proteins (50), these residues may provide ubiquitination sites in Cln3–β-Gal. Thus, the *CDC34* and *CDC28* dependence of Cln3 degradation does not appear to be dependent on the nature of its ubiquitination sites. Cln3 is the first example of a naturally unstable protein whose degradation signal can function with heterologous ubiquitination sites.

Evidence that the Cln3 degradation signal is activated by *CDC28*-dependent phosphorylation. The degradation of a number of eukaryotic proteins appears to be activated by their phosphorylation (24, 26). Four lines of evidence suggest that the Cln3 degradation signal is recognized by the ubiquitination machinery only in its phosphorylated state. First, deletion studies indicate that the ability of fragments of the Cln3 tail to signal degradation of β-Gal is correlated with their phosphorylation (Fig. 4 and 6). Second, mutations affecting ubiquitin or Ubc enzymes, which inhibit degradation of Cln3 or Cln3–β-Gal, result in accumulation of phosphorylated forms of these proteins (Fig. 7 and 8A). Third, an amino acid substitution within a Cln3 sequence matching the Cdc28 kinase consensus site results in marked inhibition of both the phosphorylation and degradation of Cln3(404-488)–β-Gal (Fig. 9). Fourth, inactivation of Cdc28 kinase inhibits both degradation and phosphorylation of Cln3 as well as Cln3–β-Gal derivatives (Fig. 8 and 10). Although the evidence for a role of phosphorylation in degradation is more extensive for the Cln3–β-Gal fusions than for Cln3 itself, other data indicate that degradation of the two proteins proceeds through the same or a similar *CDC28*-dependent pathway.

The simplest model accounting for the *CDC28* dependence of Cln3 phosphorylation is that Cln3 is phosphorylated by the same Cdc28 protein that it activates through heterodimer formation. However, our data resolve a major determinant of *CDC28* dependence of Cln3 degradation from the cyclin box, which is thought to be required for Cdc28 binding and activation by cyclins. This finding suggests that Cdc28 kinase is capable of promoting the phosphorylation of Cln3 proteins other than (or perhaps in addition to) that by which it is activated. Such mechanisms could entail either direct phosphorylation of Cln3 by Cdc28 or indirect pathways involving other protein kinases. However, it appears that Cln3 can be directly phosphorylated by Cdc28 in vitro (48).

Role of PEST elements in the phosphorylation and degradation of Cln3. We have assessed the contribution of PEST elements to the degradation of both Cln3–β-Gal and Cln3

itself. In particular, complementary deletion analyses point to the PEST 2 element as being important for Cln3 turnover (Fig. 1, 2, and 4). This is the first example of a PEST region implicated in targeting a protein for ubiquitin-dependent degradation. However, we still do not know which features of these elements are important. It should also be noted that PEST elements are not necessary for degradation in all unstable proteins in which they are found and may have other functions. Interestingly, the consensus recognition sites of Cdc28 kinase, mitogen-activated protein (MAP) kinase, and casein kinase (22, 29, 34) are all rich in PEST residues. Thus, PEST elements might function more generally as targets for phosphorylation than for degradation. Where involved in degradation, PEST sequences may serve typically to confer phosphorylation dependence on degradation, as appears to be the case for Cln3–β-Gal. C-terminal PEST sequences are present in the other G_1 cyclins of *S. cerevisiae*, Cln1 and Cln2 (14), as well as the mammalian G_1 cyclins C, D, and E (25). Thus, PEST sequences may play a general role in the degradation of G_1 cyclins, perhaps as targets for *CDC28*-dependent phosphorylation.

Cln3 instability and the control of Start. Mitotic cyclins accumulate over the S and G_2 phases in a stable form, and are abruptly degraded after their time of action, to allow continued progression of the cell cycle (12, 39). The role of instability in Cln3 function is likely to be very different. Cln3 does not appear to be stable prior to its time of action, nor does precipitous elimination of Cln3 protein occur during normal cell cycles (47). Instead, Cln3 degradation appears to be important for timing of the onset of Cln3-dependent processes such as Start. This view is consistent with the correlation between Cln3 degradation rate and cell size (Fig. 1 to 3).

The instability of Cln3 may allow its levels to reflect sensitively the immediate rate of protein synthesis in the cell, which appears to be important for the execution of Start. This model suggests that Cln3 levels should be regulated not in a temporal fashion but as a function of growth conditions. For example, at low growth rates, phosphorylation of Cln3 may be inhibited, resulting in stabilization and accumulation of Cln3 to the level critical for commitment to cell division. Control over Cln3 levels may be achieved through coupling degradation to phosphorylation. In particular, the dependence of Cln3 turnover on Cdc28 kinase provides a mechanism by which cell cycle regulators such as Cln1 and Cln2 could affect Cln3 stability. Inhibitors of Cdc28, such as Far1 (27, 46) and Sic1 (28, 32), are also interesting candidates for such regulation.

ACKNOWLEDGMENTS

We thank J. Fernando for technical assistance; M. Tyers for helping to initiate this work; G. Tokiwa and M. Sherman for advice and assistance; K. Arndt, F. Cross, C. DiComo, S. Jentsch, E. Johnson, D. Kornitzer, A. Varshavsky, D. Wolf, and T. Zhong for generously supplying strains and plasmids; F. Solomon for antitubulin antibodies; and E. Elion for discussions.

This work was supported by grants from the NIH and the Lucille P. Markey Charitable Trust (D.F.), the Human Frontier Science Program (B.F.), and NIH fellowships (M.H.L.K., D.M.R., and S.S.).

REFERENCES

1. **Amon, A., S. Irniger, and K. Nasmyth.** 1994. Closing the cell cycle circle in yeast: G_2 cyclin proteolysis initiated at mitosis persists until the activation of G_1 cyclins in the next cell cycle. Cell **77:**1037–1050.
2. **Bachmair, A., D. Finley, and A. Varshavsky.** 1986. In vivo half-life of a protein is a function of its amino-terminal residue. Science **234:**179–186.
3. **Chau, V., J. Tobias, A. Bachmair, D. Marriot, D. J. Ecker, D. K. Gonda, and A. Varshavsky.** 1989. A multiubiquitin chain is confined to a specific lysine in a targeted short-lived protein. Science **243:**1576–1583.
4. **Cross, F.** 1988. *DAF1*, a mutant gene affecting size control, pheromone arrest, and cell cycle kinetics of *Saccharomyces cerevisiae*. Mol. Cell. Biol. **8:**4675–4684.
5. **Cross, F. R., and C. M. Blake.** 1993. The yeast Cln3 protein is an unstable activator of Cdc28. Mol. Cell. Biol. **13:**3266–3271.
6. **Dou, Q.-P., A. H. Levin, S. Zhao, and A. B. Pardee.** 1993. Cyclin E and cyclin A as candidates for the restriction point protein. Cancer Res. **53:**1493–1497.
7. **Field, J., J. Nikawa, D. Broek, B. MacDonald, L. Rogers, I. A. Wilson, R. A. Lerner, and M. Wigler.** 1988. Purification of a RAS-responsive adenylyl cyclase complex from *Saccharomyces cerevisiae* by use of an epitope addition method. Mol. Cell. Biol. **8:**2159–2165.
8. **Finley, D., and V. Chau.** 1991. Ubiquitination. Annu. Rev. Cell Biol. **7:**25–69.
9. **Finley, D., E. Özkaynak, and A. Varshavsky.** 1987. The yeast polyubiquitin gene is essential for resistance to high temperatures, starvation, and other stresses. Cell **48:**1035–1046.
10. **Finley, D., S. Sadis, B. P. Monia, P. Boucher, D. J. Ecker, S. T. Crooke, and V. Chau.** 1994. Inhibition of proteolysis and cell cycle progression in a multiubiquitination-deficient yeast mutant. Mol. Cell. Biol. **14:**5501–5509.
11. **Gietz, R. D., and A. Sugino.** 1988. New yeast-Escherichia coli shuttle vectors constructed with in vitro mutagenized yeast genes lacking six-base pair restriction sites. Gene **74:**527–534.
12. **Glotzer, M., A. W. Murray, and M. W. Kirschner.** 1991. Cyclin is degraded by the ubiquitin pathway. Nature (London) **349:**132–138.
13. **Goebl, M., J. Yochem, S. Jentsch, J. P. McGrath, A. Varshavsky, and B. Byers.** 1988. The yeast cell cycle gene *CDC34* encodes a ubiquitin-conjugating enzyme. Science **241:**1331–1335.
14. **Hadwiger, J. A., C. Wittenberg, H. E. Richardson, M. de Barros Lopes, and S. I. Reed.** 1989. A family of cyclin homologs that control the G_1 phase in yeast. Proc. Natl. Acad. Sci. USA **86:**6255–6259.
15. **Heinemeyer, W., J. A. Kleinschmidt, J. Saidowsky, C. Escher, and D. Wolf.** 1991. Proteinase yscE, the yeast proteasome/multicatalytic-multifunctional proteinase: mutants unravel its function in stress induced proteolysis and uncover its necessity for cell survival. EMBO J. **10:**555–562.
16. **Hershko, A., and A. Ciechanover.** 1992. The ubiquitin system for protein degradation. Annu. Rev. Biochem. **61:**761–807.
17. **Hershko, A., D. Ganoth, V. Sudakin, A. Dahan, L. H. Cohen, F. C. Luca, J. V. Ruderman, and E. Eytan.** 1994. Components of a system that ligates cyclin to ubiquitin and their regulation by the protein kinase cdc2. J. Biol. Chem. **269:**4940–4946.
18. **Hilt, W., C. Enenkel, A. Gruhler, T. Singer, and D. H. Wolf.** 1993. The *PRE4* gene codes for a subunit of the yeast proteasome necessary for peptidylglutamyl-peptide-hydrolyzing activity. J. Biol. Chem. **268:**3479–3486.
19. **Hochstrasser, M., and A. Varshavsky.** 1990. In vivo degradation of a transcriptional regulator: the yeast α2 repressor. Cell **61:**697–708.
20. **Hodgins, R. W., K. S. Ellison, and M. J. Ellison.** 1992. Expression of a ubiquitin derivative that conjugates to protein irreversibly produces phenotypes consistent with a ubiquitin deficiency. J. Biol. Chem. **267:**8807–8812.
21. **Jentsch, S.** 1992. The ubiquitin-conjugation system. Annu. Rev. Genet. **26:**177–205.
22. **Kennelly, P. K., and E. G. Krebs.** 1991. Consensus sequences as substrate specificity determinants for protein kinases and protein phosphatases. J. Biol. Chem. **266:**15555–15558.
23. **Koch, C., and K. Nasmyth.** 1994. Cell cycle regulated transcription in yeast. Curr. Opin. Cell Biol. **6:**451–459.
24. **Kornitzer, D., B. Raboy, G. Kulka, and G. R. Fink.** Regulated degradation of the transcription factor Gcn4. EMBO J., in press.
25. **Lew, D. J., V. Dulic, and S. I. Reed.** 1991. Isolation of three novel human cyclins by rescue of G1 cyclin (Cln) function in yeast. Cell **66:**1197–1206.
26. **Lin, W.-C., and S. Desidero.** 1993. Regulation of V(D)J recombination activator protein RAG-2 by phosphorylation. Science **260:**953–959.
27. **McKinney, J. D., F. Chang, N. Heintz, and F. R. Cross.** 1993. Negative regulation of Far1 at the Start of the yeast cell cycle. Genes Dev. **7:**833–843.
28. **Mendenhall, M. D.** 1993. An inhibitor of $p34^{CDC28}$ protein kinase activity from *Saccharomyces cerevisiae*. Science **259:**216–219.
29. **Moreno, S., and P. Nurse.** 1990. Substrates for $p34^{cdc2}$: in vivo veritas? Cell **61:**549–551.
30. **Nash, R., G. Tokiwa, S. Anand, K. Erickson, and A. B. Futcher.** 1988. The $WHI1^+$ gene of *Saccharomyces cerevisiae* tethers cell division to cell size and is a cyclin homolog. EMBO J. **7:**4335–4346.
31. **Nasmyth, K.** 1993. Control of the yeast cell cycle by the Cdc28 protein kinase. Curr. Opin. Cell Biol. **5:**166–179.
32. **Nugroho, T. T., and M. D. Mendenhall.** 1994. An inhibitor of yeast cyclin-dependent protein kinase plays an important role in ensuring the genomic integrity of daughter cells. Mol. Cell. Biol. **14:**3320–3328.
33. **Pardee, A. B.** 1974. A restriction point for control of normal animal cell proliferation. Proc. Natl. Acad. Sci. USA **71:**1286–1290.
34. **Pearson, R. B., and B. E. Kemp.** 1991. Protein kinase phosphorylation site sequences and consensus specificity motifs: tabulations. Methods Enzymol. **200:**62–81.
35. **Pringle, J. R., and L. H. Hartwell.** 1981. The *Saccharomyces cerevisiae* life cycle, p. 97–142. *In* J. N. Strathern, E. W. Jones, and J. R. Broach (ed.), The molecular biology of the yeast *Saccharomyces cerevisiae*. Cold Spring Harbor

Laboratory Press, Cold Spring Harbor, N.Y.
36. **Qin, S., B. Nakajima, M. Nomura, and S. M. Arfin.** 1991. Cloning and characterization of a *Saccharomyces cerevisiae* gene encoding a new member of the ubiquitin-conjugating protein family. J. Biol. Chem. **266:**15549–15554.
37. **Rogers, S., R. Wells, and M. Rechsteiner.** 1986. Amino acid sequences common to rapidly degraded proteins: the PEST hypothesis. Science **234:**364–368.
38. **Rose, M. D., F. Winston, and P. Hieter.** 1990. Methods in yeast genetics. Cold Spring Harbor Press, Cold Spring Harbor, N.Y.
39. **Ruderman, J., F. Luca, E. Shibuya, K. Gavin, T. Boulton, and M. Cobb.** 1991. Control of the cell cycle in early embryos. Cold Spring Harbor Symp. Quant. Biol. **56:**495–502.
40. **Sambrook, J., E. F. Fritsch, and T. Maniatis.** 1989. Molecular cloning: a laboratory manual, 2nd ed. Cold Spring Harbor Press, Cold Spring Harbor, N.Y.
41. **Schwob, E., T. Bohm, M. D. Mendenhall, and K. Nasmyth.** 1994. The B-type cyclin kinase inhibitor $p40^{SIC1}$ controls the G_1 to S transition in *Saccharomyces cerevisiae*. Cell **79:**233–244.
42. **Seufert, W., and S. Jentsch.** 1990. Ubiquitin-conjugating enzymes UBC4 and UBC5 mediate selective degradation of short-lived and abnormal proteins. EMBO J. **9:**543–550.
43. **Seufert, W., and S. Jentsch.** 1992. In vivo function of the proteasome in the ubiquitin pathway. EMBO J. **11:**3077–3080.
44. **Stewart, E., H. Kobayashi, D. Harrison, and T. Hunt.** 1994. Destruction of *Xenopus* cyclins A and B2, but not B1, requires binding to $p34^{cdc2}$. EMBO J. **13:**584–594.
45. **Sudbery, P. E., A. R. Goodey, and B. L. A. Carter.** 1980. Genes which control cell proliferation in the yeast *Saccharomyces cerevisiae*. Nature (London) **288:**401–404.
46. **Tyers, M., and B. Futcher.** 1993. Far1 and Fus3 link the mating pheromone signal transduction pathway to three G_1-phase Cdc28 kinase complexes. Mol. Cell. Biol. **13:**5659–5669.
47. **Tyers, M., G. Tokiwa, and B. Futcher.** 1993. Comparison of the *Saccharomyces cerevisiae* G_1 cyclins: Cln3 may be an upstream activator of Cln1, Cln2 and other cyclins. EMBO J. **12:**1955–1968.
48. **Tyers, M., G. Tokiwa, R. Nash, and B. Futcher.** 1992. The Cln3-Cdc28 kinase complex of *S. cerevisiae* is regulated by proteolysis and phosphorylation. EMBO J. **11:**1773–1784.
49. **van der Helden, H. M. W., and M. J. Lohka.** 1994. Cell cycle-regulated degradation of *Xenopus* cyclin B2 requires binding to $p34^{cdc2}$. Mol. Biol. Cell **5:**713–724.
50. **Varshavsky, A.** 1992. The N-end rule. Cell **69:**725–735.
51. **Warner, J. R.** 1991. Labeling of RNA and phosphoproteins in *Saccharomyces cerevisiae*. Methods Enzymol. **194:**423–428.
52. **Wittenberg, C., K. Sugitomo, and S. I. Reed.** 1990. G_1-specific cyclins of *S. cerevisiae*: cell cycle periodicity, regulation by mating pheromone, and association with $p34^{CDC28}$ protein kinase. Cell **62:**225–237.